[CANCER RESEARCH 61, 8617–8623, December 15, 2001]

Advances in Brief

Cyclooxygenase-2 Is Up-Regulated in Proliferative Inflammatory Atrophy of the Prostate, but not in Prostate Carcinoma[1]

Shan Zha, Wesley R. Gage, Jurga Sauvageot, Elizabeth A. Saria, Mathew J. Putzi, Charles M. Ewing, Dennis A. Faith, William G. Nelson, Angelo M. De Marzo,[2] and William B. Isaacs

Graduate Program of Pharmacology and Molecular Sciences [S. Z], Brady Urological Institute [J. S., C. M. E., D. A. F., W. G. N., W. B. I.], and Department of Pathology [W. R. G., E. A. S., M. J. P., A. M. D.], Johns Hopkins University School of Medicine, Baltimore, Maryland 21287

Abstract

Cyclooxygenase-2 (COX-2) is the inducible isoform of the rate-limiting enzymes that convert arachidonic acid to proinflammatory prostaglandins as well as a primary target for nonsteroidal anti-inflammatory drugs. Accumulating evidence suggests that up-regulation of COX-2 is associated with carcinogenesis in multiple organ systems including the large bowel, lung, breast, and prostate. In this report, we examine the expression of COX-2 protein and mRNA in prostate tissue containing various lesions and in prostate cancer cell lines. In the cell lines, LNCaP, DU145, PC-3, and TSU, COX-2 protein expression was undetectable under basal conditions but could be induced transiently by phorbol ester treatment in PC-3 and TSU cells, but not in DU145 and LNCaP cells. Immunohistochemical analysis of 144 human prostate cancer cases suggested that, in contrast to several previous reports, there was no consistent overexpression of COX-2 in established prostate cancer or high-grade prostatic intraepithelial neoplasia, as compared with adjacent normal prostate tissue. Positive staining was seen only in scattered cells (<1%) in both tumor and normal tissue regions but was much more consistently observed in areas of proliferative inflammatory atrophy, lesions that have been implicated in prostatic carcinogenesis. Staining was also seen at times in macrophages. Western blotting and quantitative RT-PCR analyses confirmed these patterns of expression. These results suggest that if nonsteroidal anti-inflammatory drugs are indeed chemopreventive and/or chemotherapeutic for prostate cancer, their effects are likely to be mediated by modulating COX-2 activity in non-PCa cells (either inflammatory cells or atrophic epithelial cells) or by affecting a COX-2-independent pathway.

Introduction

COX[3], also called prostaglandin H_2 synthase or PGHS, is the rate-limiting enzyme for converting arachidonic acid to various proinflammatory prostaglandins. Two COX enzymes with similar catalytic features but different expression patterns have been cloned (1). COX-1 is expressed constitutively in a variety of tissues; in contrast, COX-2 is typically undetectable in most tissues but can be induced rapidly by proinflammatory signals, bacterial endotoxin, and some growth factors (2).

Research focusing on the tumor-promoting effects of COX-2 was stimulated by epidemiological studies, which have suggested that regular use of aspirin or other NSAIDs could significantly decrease the risk of developing colorectal cancer (3). The best-studied pharmacological targets for NSAIDs are the COX enzymes. COX-2, but not COX-1, has been shown to be up-regulated in transformed cells and malignant tissues, particularly in the large intestine (4). Importantly, in a murine model of familial adenomous polyposis, mice carrying $APC^{\Delta 716}$ showed marked reductions in the size and number of intestinal polyps and delayed onset of colorectal carcinoma when crossed with *COX-2* gene knockout mice (5). Recent studies on the effect of COX-2 in tumorigenesis have gone beyond colorectal cancer. Up-regulation of COX-2 has been reported in small cell lung cancer (6), breast cancer (7), skin cancer (8), and bladder cancer (9). The proposed underlying mechanisms by which COX-2 up-regulation promotes carcinogenesis include promoting angiogenesis (10), enhancing cellular motility (11), and increasing resistance to apoptosis (12).

The expression and function of COX-2 in prostate tissues and prostate cancer has been the subject of multiple recent reports (13–18). In general, the results of these studies suggest that COX-2 expression in normal prostate tissue is either weak or nonexistent and that prostate cancer tissue shows a marked overexpression of COX-2. However, a consensus has not been reached concerning which cell types express COX-2 in the prostate and at which stage of the disease its expression becomes elevated. Similarly, the extent of COX-2 expression in prostate cancer cell lines also remains unclear. Although these cell lines are generally sensitive to NSAIDs, which induce growth arrest and apoptosis (19, 20), only limited information is available concerning COX-2 expression in these lines. NSAIDs have shown promising chemoprotective and therapeutic effects against prostate cancer in animal models (21) and in humans (22) and are being tested further in clinical trials for prostate cancer prevention and therapy. To accurately assess the molecular pathways by which COX inhibitors may prevent prostate cancer, and to explain the results of clinical trials involving COX-2 inhibitors, a better understanding of the level and location of COX-2 expression in normal prostate and various prostatic lesions is critical.

Although several papers have suggested that COX-2 expression is elevated markedly in the epithelial cells in colorectal adenomas and carcinomas (23), recent immunohistochemical studies have indicated that in adenomas (polyps), expression is very weak in the epithelium but very intense in adjacent macrophages in the lamina propria (24). In a related study, Oshima *et al.* (5) showed that the *COX-2* gene promoter is active only in the lamina propria of small intestinal adenomas in *COX-2* knockout mice carrying a *COX-2* promoter-LacZ reporter construct. These findings raise the possibility that the mechanism of COX-2 inhibition of colorectal carcinogenesis involves the inhibition of inflammatory cell function. Long-standing chronic inflammation, the hallmark of which is the activated macrophage, has been linked to carcinogenesis in several organ systems including the colon (25, 26).

Received 8/6/01; accepted 10/30/01.

The costs of publication of this article were defrayed in part by the payment of page charges. This article must therefore be hereby marked *advertisement* in accordance with 18 U.S.C. Section 1734 solely to indicate this fact.

[1] Supported by USPHS Grants CA58236 and CA78588 and by an award from the Charlotte Geyer Foundation (to A. M. D.).

[2] To whom requests for reprints should addressed, at Department of Pathology, Division of Genitourinary Pathology, Bunting/Blaustein Cancer Research Building, Room 153 1650 Orleans Street, Baltimore, MD 21231-1000. Phone: (410) 614-5686; Fax: (410) 502-5158; E-mail: ademarz@jhmi.edu.

[3] The abbreviations used are: COX, cyclooxygenase; NSAID, nonsteroidal anti-inflammatory drug; RT, reverse transcription; PIA, proliferative inflammatory atrophy; PSA, prostate-specific antigen; PIN, prostate intraepithelial neoplasia; TMA, tissue microarray; PMA, phorbol 12-myristate 13-acetate; TBP, TATA-binding protein; HGPIN, high-grade PIN; PCa, prostatic adenocarcinoma.

Various focal atrophic lesions involving prostatic epithelium have been documented, described by a diverse range of terminology (27). Recently, Ruska and Epstein (28) simplified the terminology of these lesions, referring to them as simple atrophy or post atrophic hyperplasia. To emphasize the fact that these lesions tend to be highly proliferative and usually associated with inflammation, we introduced the term proliferative inflammatory atrophy, or PIA. Both Franks (29) and Liavag (30) postulated that at least some forms of atrophy were neoplastic precursors in the prostate. Recent morphological (31, 32) and genetic (33) evidence has provided preliminary support for this concept. For example, the expression of glutathione *S*-transferase π and α, enzymes that are inducible under conditions of oxidative or electrophilic stress, is elevated in PIA (31, 34). Because COX-2 is also a stress-inducible enzyme and plays a central role in the inflammatory reaction, it would be interesting to examine the expression of COX-2 in PIA and explore the potential effect of NSAIDs on the suppression of general inflammation in the prostate.

To address these questions, we conducted Western blotting and immunohistochemical analyses, using three different commercially available antibodies, in four prostate cancer cell lines and a large set of clinical prostate samples. In Western blots, COX-2 protein was at or under the detection limit under basal conditions in prostate cancer cell lines (LNCaP, DU145, PC-3, and TSU) and could be induced transiently by phorbol ester in PC-3 and TSU, but not in DU145 and LNCaP. By using immunohistochemistry, we observed a very low expression of COX-2 in both normal prostate and prostate cancer, with the exception of atrophic lesions and epithelium associated with inflammation. Quantitative RT-PCR and Western blot analysis of additional prostate tissues further confirmed these results. These studies indicate a limited role of COX-2 in established prostate cancer but suggest that COX-2 expression may contribute to the process of prostate carcinogenesis through up-regulation in PIA.

Materials and Methods

Human Tumor Specimens, Cell Lines, and Antibodies. For Northern blotting, Western blotting, and quantitative RT-PCR analysis, fresh tissue was harvested from primary tumors from patients undergoing prostatectomy at Johns Hopkins Hospital for the treatment of prostate cancer. The human prostate cancer cell lines-LNCaP, DU145, PC-3, and the human colorectal cancer cell line LOVO were acquired from the American Type Culture Collection (Manassas, VA). The human prostate cancer cell line TSU was obtained from Dr. John Isaacs at Johns Hopkins University. All cell lines were maintained in RPMI 1640 and 10% fetal bovine serum (Life Technologies, Inc., Grand Island, NY) at 37°C and 5% CO_2.

The antihuman COX-2 polyclonal rabbit antibody (PG27) from Oxford Biomedical Research, Inc. (Oxford, MI) was used for most analyses. Other antihuman COX-2 antibodies used in this study were goat polyclonal antibody from Santa Cruz Biotechnology, Inc. (N-20:sc1746; Santa Cruz, CA) and a mouse monoclonal antibody from Cayman Chemical (Ann Arbor, MI). The secondary antibodies used for Western blotting were peroxidase-conjugated donkey antirabbit IgG and goat antimouse IgG from Pierce Chemical Company (Rockford, IL). Anti-α-tubulin mouse monoclonal antibody (used as 1:4000 in Western blot) was from Oncogene Research Products (Boston, MA) and anti-PSA rabbit polyclonal antibody (used as 1:500 in Western blot) and anti-CD68 (KP-1) mouse monoclonal antibody (used as 1:2000 in immunohistochemistry) were from DAKO Corp. (Carpinteria, CA).

Immunohistochemistry. Manual immunohistochemistry was performed with the ChemMate Detection System (Ventana, Tucson, AZ) using rabbit polyclonal anti-COX-2 antibody (diluted 1: 1000; Oxford). After paraffin removal and hydration, slides were immersed in 10 mM citrate buffer (pH 6.0) and steamed for 14 min to induce epitope retrieval. Slides were incubated with primary antibodies overnight at 4°C, washed with PBS, and then incubated with secondary biotin-labeled antibodies for 30 min at room temperature. For localization, avidin-biotin complex conjugated with horseradish peroxidase was applied for 30 min at room temperature, followed by peroxide/diaminobenzidine as substrate/chromagen. The slides were counterstained with hematoxylin. To determine the potential role of background staining attributable to endogenous biotin, we used the non-biotin-based Envision Plus kit (DAKO) for anti-COX-2 staining on a number of specimens following the manufacturer's protocol (data not shown).

In a subset of specimens, a stereological grid point counting method was used to quantify the degree of immunohistochemical staining observed. This approach used a microscope eyepiece graticule (Weibel, type II) to generate an area fraction estimate of staining based upon evaluation of the individual cells on which the tip of the grid line landed (34). An area fraction of cells staining positively was obtained by determining the ratio of positively stained cells to the total number of cells counted. Areas of normal epithelium, PIA, PIN, and prostate cancer were individually identified and counted. For each different area, 30–100 cells were counted, requiring a minimum of 10 medium-power fields (×200 magnification; Olympus BX-40 microscope). The percentage of positively stained cells for each different area was generated and compared using the Kruskal-Wallis nonparametric test, followed by further analysis with Wilcoxon's rank-sum test (Stata 6.0 software; Stata Corporation, College Station, TX).

TMA Construction. A total of 121 radical prostatectomy specimens from patients with a median age of 57 (range, 37–70) were selected randomly from a total of >400 cases of prostatectomies performed between October 2000 and March 2001 at Johns Hopkins Hospital and were used to construct TMAs. Final tumor Gleason scores and stages are summarized in Table 1.

Radical prostatectomy specimens were obtained fresh from the operating room. Specimens were inked immediately, processed by a vigorous injection of formalin followed by microwave treatment, and sectioned (35). Tissues were then further fixed for 1–4 h and subjected to standard tissue processing for paraffin embedding. Final pathological slides were then used as templates for constructing three high-density TMAs with a total of 875 samples (cores, 0.6 mm in diameter) from 121 patients using a manual Tissue Puncher/Arrayer (Beecher Instruments, Silver Spring, MD) as described previously (36). Areas representing the largest carcinoma present as well as areas of normal-appearing prostate epithelium were circled on the glass slides. Each array block also contained up to 80 control normal human tissues. The TMA blocks were sectioned at 4 μm and immunostained as above for COX-2.

Once stained, the TMA slides were scanned using the BLISS imaging system as described by Manley *et al.*(37). Each array spot was then formed into a composite image that was imported into Microsoft Access 2000 for viewing. Images were viewed on the computer screen (Dell Dimension XPS 933 computer running Windows 2000, with a NEC MultiSyn FP1350 monitor) and the score (estimated percentage of positively staining cells regarding the tissue in question) was directly entered into the Microsoft Access 2000 data form. The data were then linked through a query to the clinical and pathological information. Data were then further summarized in Stata 6.0 for Microsoft Windows.

Immunoblot. Twenty-four h after being plated into 60-mm dishes, cells at 60–80% confluence were incubated for 6 h with PMA (Sigma-Aldrich, St. Louis, MO; concentrations ranged from 0–80 nM) dissolved in DMSO. Cells were then washed with PBS and lysed in a buffer containing 0.01 M Tris-HCl (pH 7.0), 1.0 mM EDTA, 0.15 M NaCl, and 4% SDS. The lysates were sonicated for 10 s on ice. The total protein concentration in each sample was measured by using bicinchoninic acid (Pierce), and 50 μg of protein was subjected to SDS-PAGE (10%), transferred to nitrocellulose (Amersham Biosciences, Inc., Piscataway, NJ), probed with antibody, and detected using enhanced chemiluminescence (Amersham).

RT and Quantitative RT-PCR. Total RNA was extracted with Trizon (Life Technologies) following the manufacturer's protocol. Total RNA (5 μg) was treated with DNase I (Life Technologies) and used to generate cDNA with

Table 1 *Pathological and clinical information of 744 cases in TMA*

Gleason score	pStage (new)			Total
	T2N0MX	T3AN0MX	T3BN0MX	
5	1	0	0	1
6	56	16	0	72
7	32	14	0	46
8	0	1	1	2
Total	89	31	1	121

SuperScript II (Life Technologies) at 46°C for 1 h, using oligo$(dT)_{12–18}$ as primers. cDNA was further treated with RNase H (Life Technologies) and used as the template for PCR.

Quantitative PCR was carried out with SYBR Green I dye (Molecular Probes, Inc., Eugene, OR). The PCR products were detected directly by measuring the increase in fluorescence caused by the binding of SYBR Green I dye to gene-specific, amplified, double-stranded DNA. The PCR primers used for COX-2 were 5′-ATGCTGAAGCCCTATGAATCA-3′ and 5′-GCCGAGGCTTTTCTACCAGA-3′; for TBP, 5′-CACGAACCACGGCACTGATT-3′ and 5′-TTTTCTTGCTGCCAGTCTGGAC-3′; and for PSA, 5′-ATGCTGCTCCGCCTGTCAG-3′ and 5′-CTTTCCCCTCAAGAACTCCTCTGG-3′. The 25-μl PCR reaction mixture contained 2.5 μl of 10X PCR buffer (magnesium concentration, 1.5 mM for COX-2, 3.0 mM for TBP, and 1.5 mM for PSA), 1 mM dNTP mixture, 0.125 μl of 5XSYBR Green I, 1 μM forward and reverse PCR primers, and 0.5 unit of Platinum Taq DNA polymerase (Life Technologies) The PCR conditions were: (*a*) 95°C for 5 min; (*b*) 95°C for 15 s; (*c*) annealing for 30 s at 57°C for COX-2 and TBP and 62.3°C for PSA; and (*d*) 72°C extension for 20 s. Fluorescence measurements were made on the ABI PRISM 7700 Sequence Detection system (PE Applied Biosystems, Forster City, CA); all measurements were performed in triplicate. COX-2, TBP, and PSA were amplified independently. TBP and PSA were measured as a reference for total RNA input and epithelial percentage of tissue samples, respectively. Standard curves for TBP, COX-2, and PSA were generated independently by serial dilutions of plasmid DNA containing corresponding amplicons. The TBP control vector was a generous gift from Dr. Arnold J. Berk (University of California, Los Angeles). The COX-2 and PSA control vectors were generated by cloning amplicons into TOPO PCRII vector (Invitrogen, Carlsbad, CA). For this purpose, each dilution was correlated with its threshold cycle, *i.e.*, the cycle number when a given sample became positive defined as a measured fluorescence at least 10 SDs above the background fluorescence. The amounts of COX-2 and PSA transcripts were normalized with TBP and presented as the ratio of COX-2 (or PSA):0.01 TBP in Fig. 4. One-hundredth TBP copy number instead of one TBP copy number was used as the denominator to facilitate the analysis by giving each data point a positive logarithm score.

Northern Blot. 20 μg of total RNA from each sample was used in Northern blot analysis, following established methods. The probes encompassing the entire open reading frame of COX-2 or β-actin were generated by RT-PCR and labeled with P^{32} using a Random Priming kit (Life Technologies). Hybridization was performed with ULTRAhyb (Ambion Inc., Austin, TX) following the manufacturer's protocol.

Results

Inducible Isogenic Cell Line Controls for COX-2 Immunohistochemical Staining. To develop and validate a immunohistochemical staining procedure for COX-2 protein expression in formalin-fixed, paraffin-embedded tissues, we first sought to use isogenic cell lines to establish positive and negative controls by Western blotting that could then be used as positive and negative controls for immunohistochemistry. We therefore determined the relative expression level of COX-2 in four human prostate cancer cell lines using the PG27 rabbit polyclonal antibody. COX-2 protein was below or at the level of detection in prostate cancer cell lines (LNCaP, DU145, PC-3, and TSU) at basal conditions (Fig. 1). Fig. 1*D* shows that under these experimental conditions, PG27 detects as little as 1 ng of recombinant COX-2 protein. Treatment of PC-3 and TSU cells with PMA resulted in dose-dependent induction of a single band migrating at ~80,000 Da, consistent with the reported apparent molecular weight of COX-2 as a glycoprotein and the electrophoretic mobility of the recombinant protein (Fig. 1). In contrast to the results obtained for PC-3 and TSU, no detectable COX-2 protein was observed in LNCaP and DU145 after PMA (80 nM) treatment (Fig. 1). COX-2 mRNA expression, as detected by Northern blotting, mirrored the protein expression detected by Western blotting (Fig. 1). An additional commercial anti-COX-2 antibody (goat polyclonal; Santa Cruz Biotechnology) gave similar results by Western blotting. A third antibody (mouse monoclonal; Cayman) showed the ~80,000-Da band and an additional band migrating at ~70,000 Da in Western blotting. The ~80,000-Da band was diminished by preincubating the primary antibody with blocking peptide (5 μg/ml; Cayman), but not the ~70,000-Da band. Therefore, the reactivity against the ~70,000-Da band was considered nonspecific (data not shown).

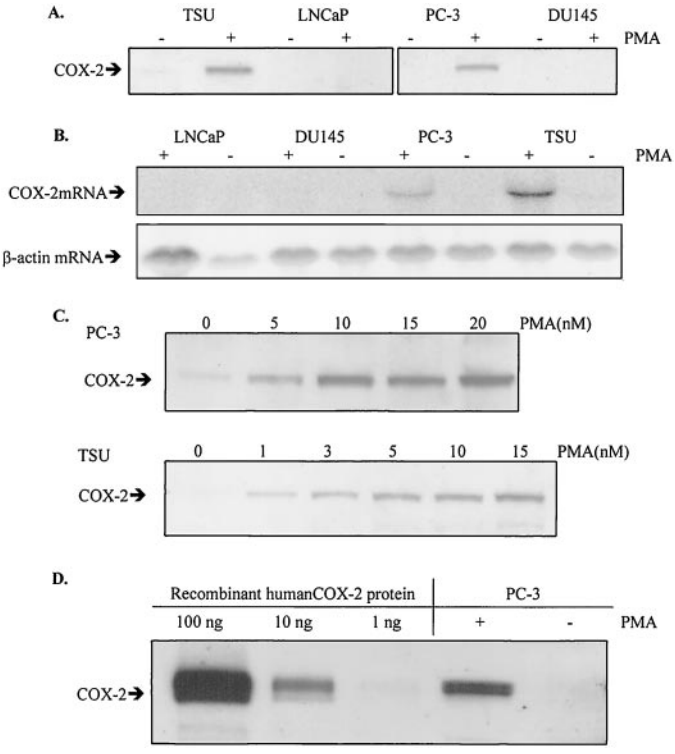

Fig. 1. COX-2 expression in prostate cancer cell lines-LNCaP, DU145, PC-3, and TSU. *A*, Western analysis of COX-2 protein in TSU, DU145, PC-3, and LNCaP cell lines with or without PMA induction (80 nM, 6 h). *B*, Northern analysis of COX-2 mRNA in TSU, DU145, PC-3, and LNCap cell lines with or without PMA induction (80 nM, 6 h). *C*, Western analysis of COX-2 in PC-3 and TSU cell, induced by PMA at different concentrations for 6 h. *D*, Western analysis of COX-2 using PG27 detects 100 ng, 10 ng, and 1 ng of recombinant COX-2 protein or COX-2 in 50 μg of PC-3 cell lysate with or without PMA incubation (80 nM, 6 h).

PC-3 cells were incubated for 6 h with and without PMA (80 nM) as in Fig. 1. The cell pellets were prepared and placed in formalin. Following fixation and embedding into paraffin blocks, sections were subjected to immunohistochemical staining with the PG27 antibody. In cells without inductive PMA treatment, only light staining was seen (Fig. 2*H*, *top*). This light staining was completely eliminated by using a non-biotin-based immunohistochemical method (Envision Plus) and was thus considered background staining. Following PMA treatment, a majority of the cells showed very intense staining for COX-2 (Fig. 2*H*, *bottom*). These isogenic systems show clearly that the inducibility of COX-2, as seen by Western blotting, can also be detected by immunohistochemistry of formalin-fixed, paraffin-embedded cells. The two additional COX-2-specific commercial antibodies (Santa Cruz Biotechnology polyclonal and Cayman monoclonal) produced similar results by immunohistochemistry. Of note, at a relatively high dilution (<1:10,000), the Cayman monoclonal antibody showed a striking plasma membrane staining pattern that was completely eliminated by further dilution (up to 1:80,000) without loss of intense staining of the seminal vesicles (see below). COX-2 has not been reported previously as a cell membrane protein. Taken together with the Western blot data obtained for this antibody as described above, these observations suggest that the plasma membrane staining is most likely attributable to a cross-reaction of this antibody with a non-

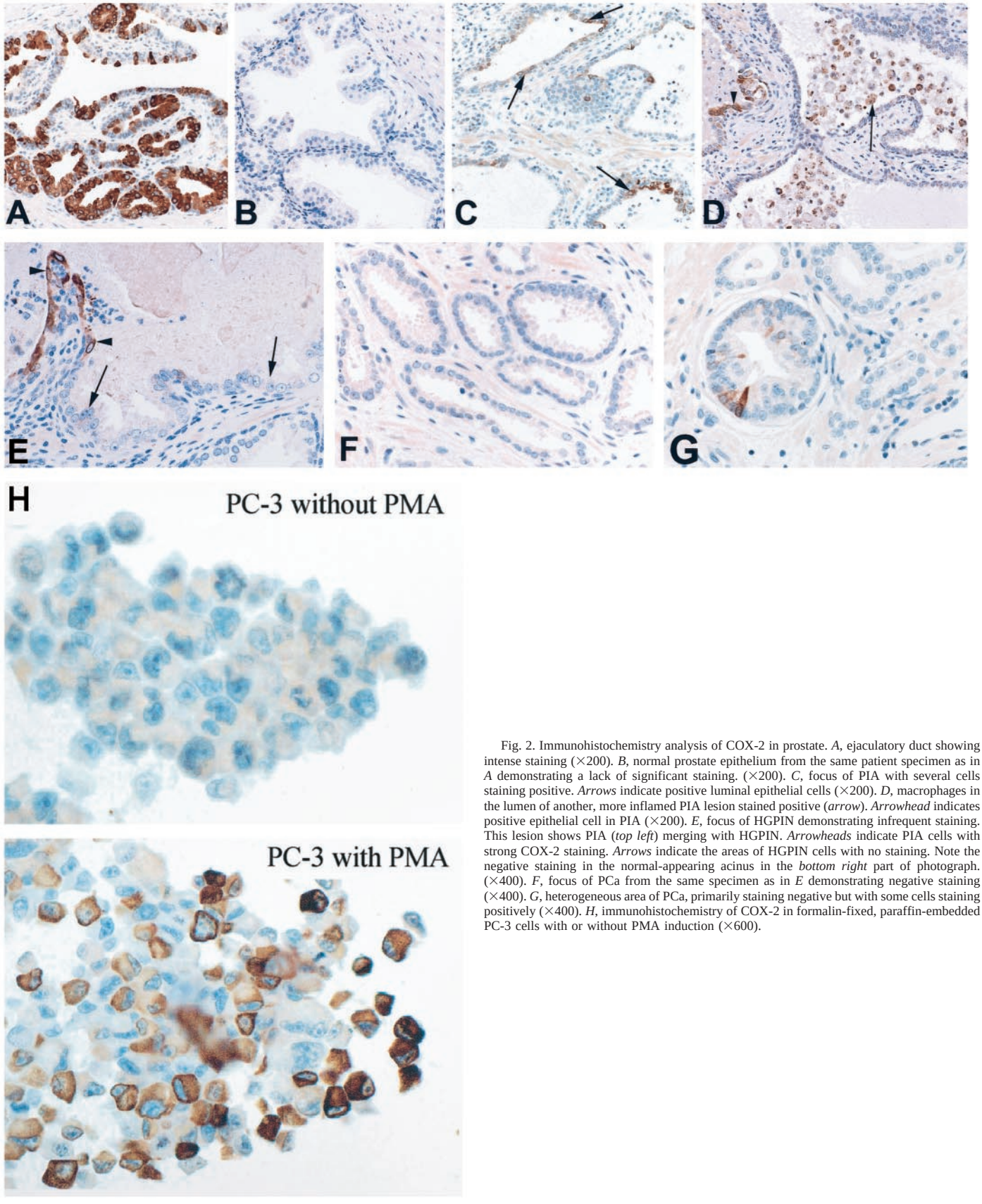

Fig. 2. Immunohistochemistry analysis of COX-2 in prostate. *A*, ejaculatory duct showing intense staining (×200). *B*, normal prostate epithelium from the same patient specimen as in *A* demonstrating a lack of significant staining. (×200). *C*, focus of PIA with several cells staining positive. *Arrows* indicate positive luminal epithelial cells (×200). *D*, macrophages in the lumen of another, more inflamed PIA lesion stained positive (*arrow*). *Arrowhead* indicates positive epithelial cell in PIA (×200). *E*, focus of HGPIN demonstrating infrequent staining. This lesion shows PIA (*top left*) merging with HGPIN. *Arrowheads* indicate PIA cells with strong COX-2 staining. *Arrows* indicate the areas of HGPIN cells with no staining. Note the negative staining in the normal-appearing acinus in the *bottom right* part of photograph. (×400). *F*, focus of PCa from the same specimen as in *E* demonstrating negative staining (×400). *G*, heterogeneous area of PCa, primarily staining negative but with some cells staining positively (×400). *H*, immunohistochemistry of COX-2 in formalin-fixed, paraffin-embedded PC-3 cells with or without PMA induction (×600).

COX-2 antigen. On the basis of these results, we chose the PG27 antihuman COX-2 antibody for use in our protocol for analysis of archival prostate tissue specimens.

Low COX-2 Expression in Normal Prostate, PIN, and Prostate Cancer. Formalin-fixed and paraffin-embedded surgical specimens from an initial 24 patients (28 slides) and an additional 121 different

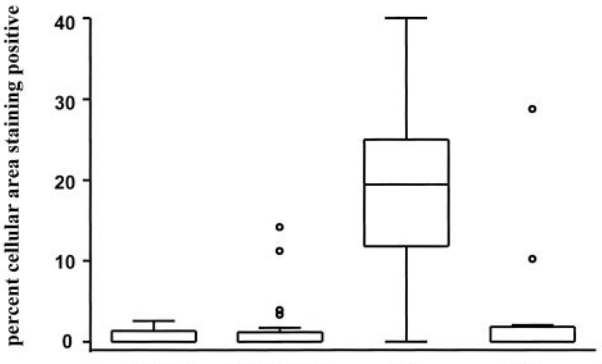

	Normal	PCa/Primary	PIA	PIN	Total
Median(%)	0	0	0	20	/
Range(%)	0-2.6	0-14.6	0-29.6	0-41.2	/
Case	19	21	11	8	23
Slide	28	24	13	11	28

Fig. 3. Quantitative analysis of COX-2 staining in prostate cancer. Quantification of COX-2 staining in normal prostate, PIA, PIN, and PCa. The *box* shows the 25th–75th percentiles as well as the median. The *bars* show the 5th and 95th percentiles, and the ○ represent outliers.

patients treated by radical prostatectomy for prostate cancer were evaluated for immunoreactive COX-2 with the PG27 antibody, using standard slides and three high-density TMAs. Immunohistochemical staining of normal prostate was negative in the vast majority of epithelial cells (Fig. 2*B*). Slight stromal staining was observed; this staining was eliminated using the non-biotin based system and was therefore considered as background. Very strong cytoplasmic staining was seen in the majority of the epithelial cells in the ejaculatory ducts (Fig. 2*A*). Because these structures, which course through the central zone of the prostate, are continuous with and identical in histology to the seminal vesicles, additional sections of seminal vesicles were stained ($n = 5$). All seminal vesicle sections showed very intense immunoreactivity generally in >50% of epithelial cells with the COX-2 antibody. This is perhaps not unexpected, as the seminal vesicle secretions of the human contain high levels of prostaglandins (38). This intense protein staining correlated well with the abundant mRNA for COX-2 detected by Northern blot and RT-PCR analysis (see Fig. 4) and provided a further verification of our COX-2 staining protocol.

In contrast, normal prostate epithelium and stroma (Fig. 2*B*) were generally negative for COX-2 staining, as were scattered collections of lymphocytes. Like normal prostate tissue, prostate cancer cells demonstrated negative or only focal, weak positive COX-2 staining (Fig. 2, *F* and *G*). Lesions of HGPIN showed similar staining to that of prostate cancer (Fig. 2*E*).

In contrast to normal prostate and prostate cancer, epithelial cells in PIA often showed a number of cells with intense COX-2 staining (Fig. 2, *C–E*). The extent of inflammation in PIA did not appear to influence the COX-2 staining in the adjacent atrophic epithelium. Mononuclear cells with the morphological appearance of macrophages (defined by immunostaining with monoclonal antibody to KP-1) within all three tissue compartments (stromal, luminal, and intraepithelial) at times showed strong COX-2 staining (Fig. 2*D*).

Because staining was heterogeneous, in order to more reliably quantify the immunohistochemical staining in normal prostate and the various lesions, in a set of 28 slides from 24 patients we used standard sections and applied a stereological grid point counting method (Ref. 34; Fig. 3). The median area fraction of cells that stained positive presented by percentage is 0 in normal prostate (range, 0–2.6), 0 in prostate cancer (range, 0–14.6), and 0 in PIN (range, 0–29.6), as shown in Fig. 3. In contrast to the lack of expression in normal prostate and prostate cancer, the median percentage of cells that stained positive in PIA was 20 (range, 0–41.2; Fig. 3). When compared with the percentage of positive cells in normal, PIN, and prostate cancer, the staining in PIA was highly significant ($\chi^2 = 19.773$ with 3 degrees of freedom; $P = 0.0002$). In this subset of cases, there was no correlation between COX-2 staining and Gleason grade (Gleason 6, $n = 9$ and Gleason 7, $n = 15$; $\chi^2 = 0.288$; and $P = 0.5915$) or between COX-2 staining and pathological stage (<T3:$n = 12$; T3:$n = 11$; Tx:$n = 1$; $\chi^2 = 0.164$; and $P = 0.6815$). Consistent with a lack of staining in prostate cancer, even in aggressive lesions, 4 of 4 metastatic PCas to pelvic lymph nodes were completely negative for COX-2 staining.

We stained an additional 121 prostate cancer cases using high-density TMAs to further verify the observation of a lack of COX-2 overexpression in prostate cancer. A total of 875 cores from these 121 patient cases were imaged by using the BLISS system. Within the 875 images analyzed for COX-2 staining, 80 had no tissue, 15 had tissue too scant to evaluate, and 36 were not interpretable because of blurry images or equivocal histology. Thus, a total of 744 images could be evaluated (85%). Table 2 shows the estimated percentage of cells in the given category that were positive for COX-2 above background staining. The results validate the findings using standard specimens, markedly expanding the number of cases analyzed. Of note, there was higher variability, which is likely the result of the more subjective nature of estimating the percentage of positive staining as opposed to the more laborious grid point counting method. Of interest, some of the tissue of which the target diagnosis was normal was found to contain HGPIN and/or PIA. In addition, there was a predilection for tumors showing focal mucinous differentiation to contain more COX-2-positive tumor cells (Table 2).

Consistent with the immunohistochemical results described above, when COX-2 protein was analyzed on nine pairs of tumor and normal tissue lysates as well as one seminal vesicle lysate by Western blotting, only 1 of the 18 prostate samples had detectable COX-2 protein (Fig. 4*C*). At the same time, the seminal vesicle lysate demonstrated a large amount of COX-2 protein (Fig. 4*C*). Northern blot analyses of COX-2 mRNA in eight independent seminal vesicle samples were consistent with this result (Fig. 4*B*).

To quantify the relative levels of COX-2 mRNA expression in the various tissues in question, we assayed COX-2 mRNA expression in prostate tissues and seminal vesicles by quantitative RT-PCR. PSA mRNA and TBP mRNA were also analyzed as markers for epithelial percentage in prostate and total RNA input, respectively. Standard curves were generated for COX-2, TBP, and PSA independently, as described in "Materials and Methods." The quantities of COX-2 and PSA were normalized to the absolute quantity of the TBP transcript. As summarized in Fig. 4, the PSA levels were slightly lower in prostate cancer than normal prostate. This finding is in agreement with prior studies (39, 40). For the same group of samples, the median levels of COX-2 transcripts were 122.79 for normal prostate (range,

Table 2 *Analysis of 744 array cores for COX-2 staining (positive stain percentage)*

Tissue	*n*	Mean (%)	SD (%)	Median (%)	Range (%)
Gleason 2	1	NA	NA	NA	NA
Gleason 3	240	0.37	1.9	0	0–20
Gleason 4	27	0.18	0.96	0	0–5
Mucinous	10	7.5	10	5	0–30
HGPIN	9	0.56	1.7	0	0–5
Normal prostate epithelial	345	0.6	5.2	0	0–80
Normal prostate stroma	77	0	0	0	0
PIA	35	17.8	16.9	10	0–70
Total	744				

NA, not available.

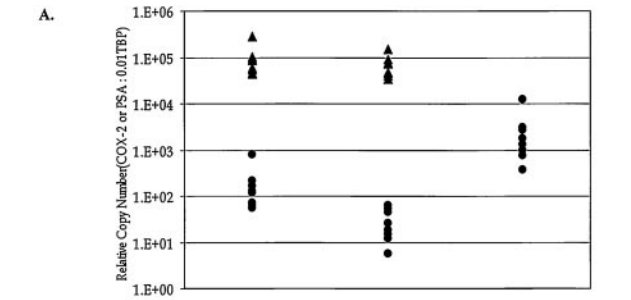

Tissue Type		Normal Prostate	Prostate Cancer	Seminal Vesicle
COX-2	Mean (ratio)	122.8	23.4	1528.6
●	Min/Max(ratio)	42.4/917.7	4.3 / 82.9	243.4 /17892.8
PSA	Mean (ratio)	72340.92	56993.4	N/A
▲	Min/Max(ratio)	21536.7/338107.1	16925.6/170895.8	N/A

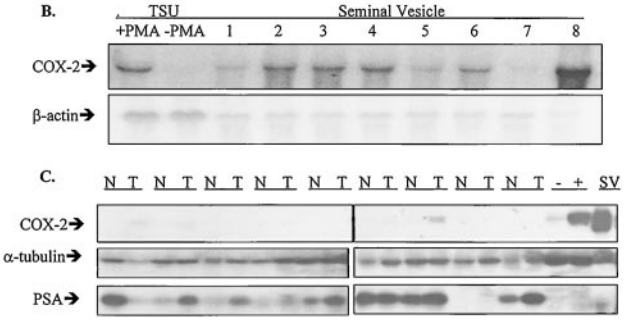

Fig. 4. Quantitative PCR, Northern blot, and Western blot analysis of COX-2 expression on frozen tissues. *A*, quantitative PCR of COX-2 and PSA expression in normal prostate, prostate cancer, and seminal vesicle. *B*, Northern blot analysis of seminal vesicle total RNA for COX-2 and β-actin. *C*, expression of COX-2 protein in prostate tissue. 50 μg of total protein from frozen tissue was subjected to electrophoresis and Western analysis for COX-2, PSA, and α-tubulin. The − and + denote the colon cancer cell line LOVO without or with PMA induction. *SV*, seminal vesicle tissue.

42.35–917.70) and 23.43 for prostate cancer (range, 4.30−82.86). These data do not support prior findings of an overexpression of COX-2 in prostate cancer and, in fact, suggest a down-regulation of COX-2 in prostate cancer. The levels of COX-2 mRNA in seminal vesicle tissue were >10-fold higher than in prostate, with the median at 1528.55 (range, 243.41–17892.8). This finding is consistent with the intense immunostaining of COX-2 that we observed in the seminal vesicles.

Discussion

Recent epidemiological studies suggest that extensive NSAID use can decrease prostate cancer risk (22). COX-2 inhibitors also decrease the extent of tumor burden in an established prostate cancer xenografts model (PC-3; Ref. 21). Clarification of the expression pattern of COX-2 in prostate tissues, therefore, is critical to deciphering the mechanisms whereby COX inhibitors may prevent and/or treat prostate cancer. A number of recent studies have examined COX-2 expression by immunohistochemistry in normal prostate and prostate cancer (13–18, 41). Because most studies published to date have concluded that there is an up-regulation of COX-2 in prostate cancer, most investigators have argued that the effects of NSAIDs on prostate cancer are likely mediated by inhibition of the function of COX-2 enzymatic activity in the prostate cancer cells. Yet, many of the observations regarding COX-2 expression in prostate tissues are difficult to resolve. Discrepancies in published reports include whether or not COX-2 is expressed in normal prostate, which cell types (*e.g.*, epithelial cells, smooth muscle cells, or stroma) express COX-2, whether COX-2 expression is elevated in PIN or prostate carcinoma, and whether the expression level of COX-2 in PCa is associated with cellular differentiation or disease progression. Despite these issues, clinical trials of prostate cancer prevention and therapy using selective COX-2 inhibitors have been initiated (21). The results presented in this study indicate that COX-2 protein is expressed at very low or undetectable levels in normal prostate and that COX-2 expression is not consistently elevated in PIN or prostate cancer. Furthermore, when staining for COX-2 was observed in prostate cancer, the extent of positive staining did not correlate with established clinical-pathological risk factors (Gleason score or pathological stage).

Because our results were in conflict with a number of recent studies in that we do not find an overexpression of COX-2 in prostate cancer, we performed a number of control experiments to verify the sensitivity and specificity of the antibodies used. First, we showed that expression of COX-2 by immunohistochemistry correlated precisely with Western blot data using isogenic cell lines that were induced to express COX-2 by phorbol ester treatment. Second, Western blot analysis performed on frozen human prostate tumor/normal pairs provided similar results. Third, three different commercial COX-2-specific antibodies produced nearly identical results (although, as described above, one of the antibodies appeared to recognize an additional antigen as well as COX-2). Fourth, expression data as determined by immunohistochemistry and Western blotting correlated with expression of mRNA by both Northern analysis and real time quantitative RT-PCR. None of the studies published previously included the performance of such rigorous quality assessments of the immunohistochemical assays used. While this report was in progress, a recent study also found low expression of COX-2 in prostate cancer (42), although they reported more COX-2 expression in higher-grade tumors.

The expression and function of COX-2 in prostate cancer cell lines was also addressed in this study by using Western and Northern blot analysis. Previous studies suggested that these cell lines are generally sensitive to NSAIDs (such as NS398 and sulindac), resulting in apoptosis. Expression of COX-2 was proposed as the target for NSAIDs (19, 20, 43). According to the results presented here, COX-2 expression is very limited in these prostate cancer cell lines, implying that NSAIDs may function through a COX-2 independent pathway. NSAID-sensitive, COX-2- negative colorectal cancer cell lines have been reported (44, 45). Indeed, COX-2 independent mechanisms of NSAID action have been identified, *e.g.*, involving peroxisome proliferative activated receptor (PPARβ or δ; Ref. 46), apoptosis proteins BAX and Bcl-XL (45), or ceramide accumulation (44).

Long-term chronic inflammation contributes to carcinogenesis in many organ systems (25, 26, 47) through a postulated mechanism of repetitive tissue damage and regeneration in the presence of free radicals and inflammatory cytokines. Increased expression of COX-2 at inflammatory sites or in the inflammatory cells has also been reported for colorectal tissues, where COX-2 has been suggested to play a synergistic role in tumorigenesis (24). The catalytic activity of COX-2 results in the production of potentially DNA-damaging free radicals (48). Overexpression of COX-2 also increases resistance to apoptosis (20). A combination of these effects, contributing to permanent damage in genomic DNA and cellular transformation, is compatible with the proposed mechanism for inflammation-related risk for cancer.

Previous morphological studies suggested that focal atrophy, which is often associated with chronic and at times acute inflammation, might be a prostate cancer precursor (29, 30). More recent studies indicate that these lesions, which we refer to as PIA, are characterized by an increased proliferative index, increased bcl-2, low apoptosis, decreased $p27^{Kip1}$, and increased expression of glutathione *S*-transferase π and α (28, 31, 34). The latter markers are typically stress-induced, which is consistent with the stress-induced expression in PIA of COX-2 found in this study. Additional data further implicates PIA in prostate carcinogenesis. For example, PIA lesions are often found to

merge with HGPIN (32), are often found in proximity to carcinoma, and have increased chromosome 8 copy number (33, 49). A potentially important implication of our results, therefore, is that NSAIDs might have chemopreventive effects on prostate cancer by controlling or minimizing carcinogenic chronic inflammation in the prostate and/or by inhibiting the proliferation of, or inducing the apoptosis of, the epithelial cells in PIA lesions themselves. The effects of NSAIDs on various prostate lesions can be assessed directly by examination of the tissues derived from surgical specimens from patients treated with these agents prior to prostatectomy. These types of studies are currently underway. Furthermore, our results indicate that because COX-2 is not overexpressed in established cancer or in HGPIN, the therapeutic effect of COX-2 inhibitors on prostate cancer, if such an effect exists, may be mediated by non-PCa cells in the prostate or by COX-2-independent pathways.

Acknowledgments

We thank Helen Fedor, Marcella Southerland, and Gerrun March for diligent construction of tissue microarrays.

References

1. Smith, W. L., DeWitt, D. L., and Garavito, R. M. Cyclooxygenases: structural, cellular, and molecular biology. Annu. Rev. Biochem., *69:* 145–182, 2000.
2. Gilroy, D. W., and Colville-Nash, P. R. New insights into the role of COX 2 in inflammation. J. Mol. Med., *78:* 121–129, 2000.
3. Sandler, R. S. Aspirin and other nonsteroidal anti-inflammatory agents in the prevention of colorectal cancer. *In:* S. Helman, S. A. Rosenberg, and V. T. DeVita (eds.) Important Advances in Oncology, pp. 123–137. Philadelphia: Lippincott-Raven, 1996.
4. Fosslien, E. Molecular pathology of cyclooxygenase-2 in neoplasia. Ann. Clin. Lab. Sci., *30:* 3–21, 2000.
5. Oshima, M., Dinchuk, J. E., Kargman, S. L., Oshima, H., Hancock, B., Kwong, E., Trzaskos, J. M., Evans, J. F., and Taketo, M. M. Suppression of intestinal polyposis in Apc δ716 knockout mice by inhibition of cyclooxygenase 2 (COX-2). Cell, *87:* 803–809, 1996.
6. Wolff, H., Saukkonen, K., Anttila, S., Karjalainen, A., Vainio, H., and Ristimaki, A. Expression of cyclooxygenase-2 in human lung carcinoma. Cancer Res., *58:* 4997–5001, 1998.
7. Hwang, D., Scollard, D., Byrne, J., and Levine, E. Expression of cyclooxygenase-1 and cyclooxygenase-2 in human breast cancer. J. Natl. Cancer Inst. (Bethesda), *90:* 455–460, 1998.
8. Muller-Decker, K., Reinerth, G., Krieg, P., Zimmermann, R., Heise, H., Bayerl, C., Marks, F., and Furstenberger, G. Prostaglandin-H-synthase isozyme expression in normal and neoplastic human skin. Int. J. Cancer, *82:* 648–656, 1999.
9. Shirahama, T. Cyclooxygenase-2 expression is up-regulated in transitional cell carcinoma and its preneoplastic lesions in the human urinary bladder. Clin. Cancer Res., *6:* 2424–2430, 2000.
10. Tsujii, M., Kawano, S., Tsuji, S., Sawaoka, H., Hori, M., and DuBois, R. N. Cyclooxygenase regulates angiogenesis induced by colon cancer cells (Published erratum appears in Cell, *94:* following 271). Cell, *93:* 705–716, 1998.
11. Tsujii, M., and DuBois, R. N. Alterations in cellular adhesion and apoptosis in epithelial cells overexpressing prostaglandin endoperoxide synthase 2. Cell, *83:* 493–501, 1995.
12. Richter, M., Weiss, M., Weinberger, I., Furstenberger, G., and Marian, B. Growth inhibition and induction of apoptosis in colorectal tumor cells by cyclooxygenase inhibitors. Carcinogenesis (Lond.), *22:* 17–25, 2001.
13. Gupta, S., Srivastava, M., Ahmad, N., Bostwick, D. G., and Mukhtar, H. Overexpression of cyclooxygenase-2 in human prostate adenocarcinoma. Prostate, *42:* 73–78, 2000.
14. Kirschenbaum, A., Klausner, A. P., Lee, R., Unger, P., Yao, S., Liu, X. H., and Levine, A. C. Expression of cyclooxygenase-1 and cyclooxygenase-2 in the human prostate. Urology, *56:* 671–676, 2000.
15. Kirschenbaum, A., Liotta, D. R., Yao, S., Liu, X. H., Klausner, A. P., Unger, P., Shapiro, E., Leav, I., and Levine, A. C. Immunohistochemical localization of cyclooxygenase-1 and cyclooxygenase-2 in the human fetal and adult male reproductive tracts. J. Clin. Endocrinol. Metab., *85:* 3436–3441, 2000.
16. Madaan, S., Abel, P. D., Chaudhary, K. S., Hewitt, R., Stott, M. A., Stamp, G. W., and Lalani, E. N. Cytoplasmic induction and over-expression of cyclooxygenase-2 in human prostate cancer: implications for prevention and treatment. BJU Int., *86:* 736–741, 2000.
17. Tanji, N., Kikugawa, T., and Yokoyama, M. Immunohistochemical study of cyclooxygenases in prostatic adenocarcinoma; relationship to apoptosis and Bcl-2 protein expression. Anticancer Res., *20:* 2313–2319, 2000.
18. Yoshimura, R., Sano, H., Masuda, C., Kawamura, M., Tsubouchi, Y., Chargui, J., Yoshimura, N., Hla, T., and Wada, S. Expression of cyclooxygenase-2 in prostate carcinoma. Cancer (Phila.), *89:* 589–596, 2000.
19. Lim, J. T., Piazza, G. A., Han, E. K., Delohery, T. M., Li, H., Finn, T. S., Buttyan, R., Yamamoto, H., Sperl, G. J., Brendel, K., Gross, P. H., Pamukcu, R., and Weinstein, I. B. Sulindac derivatives inhibit growth and induce apoptosis in human prostate cancer cell lines. Biochem. Pharmacol., *58:* 1097–1107, 1999.
20. Liu, X. H., Yao, S., Kirschenbaum, A., and Levine, A. C. NS398, a selective cyclooxygenase-2 inhibitor, induces apoptosis and down-regulates bcl-2 expression in LNCaP cells. Cancer Res., *58:* 4245–4249, 1998.
21. Liu, X. H., Kirschenbaum, A., Yao, S., Lee, R., Holland, J. F., and Levine, A. C. Inhibition of cyclooxygenase-2 suppresses angiogenesis and the growth of prostate cancer *in vivo*. J. Urol., *164:* 820–825, 2000.
22. Nelson, J. E., and Harris, R. E. Inverse association of prostate cancer and nonsteroidal anti-inflammatory drugs (NSAIDs): results of a case-control study. Oncol. Rep., *7:* 169–170, 2000.
23. Fujita, M., Fukui, H., Kusaka, T., Ueda, Y., and Fujimori, T. Immunohistochemical expression of cyclooxygenase (COX)-2 in colorectal adenomas. J. Gastroenterol., *35:* 488–490, 2000.
24. Chapple, K. S., Cartwright, E. J., Hawcroft, G., Tisbury, A., Bonifer, C., Scott, N., Windsor, A. C., Guillou, P. J., Markham, A. F., Coletta, P. L., and Hull, M. A. Localization of cyclooxygenase-2 in human sporadic colorectal adenomas. Am. J. Pathol., *156:* 545–553, 2000.
25. Ames, B. N. Mutagenesis and carcinogenesis: endogenous and exogenous factors. Environ. Mol. Mutagen., *14* (Suppl.)*:* 66–77, 1989.
26. Bartsch, H., and Frank, N. Blocking the endogenous formation of *N*-nitroso compounds and related carcinogens. IARC Sci. Publ. *139:* 189–201, 1996.
27. Putzi, M. J., and De Marzo, A. M. Prostate pathology, histology and molecular perspectives. *In:* M. A. Carducci. and M. A. Eisenberger (eds.), Hematology Oncology Clinics of North America. pp. 407–421, Philadelphia: W. B. Saunders Co., 2001.
28. Ruska, K. M., Sauvageot, J., and Epstein, J. I. Histology and cellular kinetics of prostatic atrophy. Am. J. Surg. Pathol., *22:* 1073–1077, 1998.
29. Franks, L. Atrophy and hyperplasia in the prostate proper. J. Pathol. Bacteriol., *68:* 617–625, 1954.
30. Liavag, I. Atrophy and regeneration in the pathogenesis of prostatic carcinoma. Acta Pathol. Microbiol. Scand., *73:* 338–350, 1968.
31. De Marzo, A. M., Marchi, V. L., Epstein, J. I., and Nelson, W. G. Proliferative inflammatory atrophy of the prostate: implications for prostatic carcinogenesis. Am. J. Pathol., *155:* 1985–1992, 1999.
32. Putzi, M. J., and De Marzo, A. M. Morphologic transitions between proliferative inflammatory atrophy and high-grade prostatic intraepithelial neoplasia. Urology, *56:* 828–832, 2000.
33. Shah, R., Mucci, N. R., Amin, A., Macoska, J. A., and Rubin, M. A. Postatrophic hyperplasia of the prostate gland: neoplastic precursor or innocent bystander? Am. J. Pathol., *158:* 1767–1773, 2001.
34. Parsons, J. K., Nelson, C. P., Gage, W. R., Nelson, W. G., Kensler, T. W., and De Marzo, A. M. GSTA1 expression in normal, pre-neoplastic, and neoplastic human prostate tissue. Prostate, *49:* 30–37, 2001.
35. Ruijter, E. T., Miller, G. J., Aalders, T. W., van de Kaa, C. A., Schalken, J. A., Debruyne, F. M., and Boon, M. E. Rapid microwave-stimulated fixation of entire prostatectomy specimens. Biomed-II MPC Study Group. J. Pathol., *183:* 369–375, 1997.
36. Kononen, J., Bubendorf, L., Kallioniemi, A., Barlund, M., Schraml, P., Leighton, S., Torhorst, J., Mihatsch, M. J., Sauter, G., and Kallioniemi, O. P. Tissue microarrays for high-throughput molecular profiling of tumor specimens. Nat. Med., *4:* 844–847, 1998.
37. Manley S, Mucci, N. R., De Marzo, A. M., and Rubin, M. A. Relational database structure to manage high-density tissue microarray data and images for pathology studies focusing on clinical outcome: the prostate specialized program of research excellence model. Am. J. Pathol., *159:* 837–843, 2001.
38. Rui, H., Thomassen, Y., Oldereid, N. B., and Purvis, K. Accessory sex gland function in normal young (20–25 years) and middle- aged (50–55 years) men. J. Androl, *7:* 93–99, 1986.
39. Hakalahti, L., Vihko, P., Henttu, P., Autio-Harmainen, H., Soini, Y., and Vihko, R. Evaluation of *PAP* and *PSA* gene expression in prostatic hyperplasia and prostatic carcinoma using Northern-blot analyses, *in situ* hybridization and immunohistochemical stainings with monoclonal and bispecific antibodies. Int. J. Cancer, *55:* 590–597, 1993.
40. Magklara, A., Scorilas, A., Stephan, C., Kristiansen, G. O., Hauptmann, S., Jung, K., and Diamandis, E. P. Decreased concentrations of prostate-specific antigen and human glandular kallikrein 2 in malignant *versus* nonmalignant prostatic tissue. Urology, *56:* 527–532, 2000.
41. Uotila, P., Valve, E., Martikainen, P., Nevalainen, M., Nurmi, M., and Harkonen, P. Increased expression of cyclooxygenase-2 and nitric oxide synthase-2 in human prostate cancer. Urol. Res., *29:* 23–28, 2001.
42. Shappell, S. B., Manning, S, Boeglin, W. E., Guan, Y., Robert, R. L., Davis, L., Olson, S. J., Jack, G. S., Coffey, C. S., Wheeler, T. M., Breyer, M. D., and Brash, A. R. Alteration in lipoxygenase and cyclooxygenase-2 catalytic activity and mRNA expression in prostate carcinoma. Neoplasia, *3:* 287–303, 2001.
43. Hsu, A. L., Ching, T. T., Wang, D. S., Song, X., Rangnekar, V. M., and Chen, C. S. The cyclooxygenase-2 inhibitor celecoxib induces apoptosis by blocking Akt activation in human prostate cancer cells independently of Bcl-2. J. Biol. Chem., *275:* 11397–11403, 2000.
44. Chan, T. A., Morin, P. J., Vogelstein, B., and Kinzler, K. W. Mechanisms underlying nonsteroidal antiinflammatory drug-mediated apoptosis. Proc. Natl. Acad. Sci. USA, *95:* 681–686, 1998.
45. Zhang, L., Yu, J., Park, B. H., Kinzler, K. W., and Vogelstein, B. Role of BAX in the apoptotic response to anticancer agents. Science (Wash. DC), *290:* 989–992, 2000.
46. He, T. C., Chan, T. A., Vogelstein, B., and Kinzler, K. W. PPARδ is an APC-regulated target of nonsteroidal anti-inflammatory drugs. Cell, *99:* 335–345, 1999.
47. Weitzman, S. A., and Gordon, L. I. Inflammation and cancer: role of phagocyte-generated oxidants in carcinogenesis. Blood, *76:* 655–663, 1990.
48. Nikolic, D., and van Breemen, R. B. DNA oxidation induced by cyclooxygenase-2. Chem. Res. Toxicol., *14:* 351–354, 2001.
49. Macoska, J. A., Trybus, T. M., and Wojno, K. J. 8p22 loss concurrent with 8c gain is associated with poor outcome in prostate cancer. Urology, *55:* 776–782, 2000.